Author/s:
Quah, PS;Tran, BM;Corbin, VDA;Chang, JJ-Y;Wong, CY;Diaz-Méndez, A;Hartley, CA;Zeng, W;Hanssen, E;Trifunovic, Z;Reading, PC;Jackson, DC;Vincan, E;Coin, LJM;Deliyannis, G

Title:
Development of Matrix-Embedded Bovine Tracheal Organoids to Study the Innate Immune Response against Bovine Respiratory Disease

Date:
2023

Citation:
Quah, P. S., Tran, B. M., Corbin, V. D. A., Chang, J. J. -Y., Wong, C. Y., Diaz-Méndez, A., Hartley, C. A., Zeng, W., Hanssen, E., Trifunovic, Z., Reading, P. C., Jackson, D. C., Vincan, E., Coin, L. J. M. & Deliyannis, G. (2023). Development of Matrix-Embedded Bovine Tracheal Organoids to Study the Innate Immune Response against Bovine Respiratory Disease. Organoids, 2 (2), pp.82-101. https://doi.org/10.3390/organoids2020007.

Persistent Link:
https://hdl.handle.net/11343/339334

organoids

MDPI

Article

Development of Matrix-Embedded Bovine Tracheal Organoids to Study the Innate Immune Response against Bovine Respiratory Disease

Pin Shie Quah [1,†], Bang M. Tran [2,†], Vincent D.A. Corbin [1], Jessie J.-Y. Chang [1], Chinn Yi Wong [1], Andrés Diaz-Méndez [3], Carol A. Hartley [3], Weiguang Zeng [1], Eric Hanssen [4,5], Zlatan Trifunovic [4], Patrick C. Reading [1,6], David C. Jackson [1], Elizabeth Vincan [2,7,8,‡], Lachlan J.M. Coin [1,‡] and Georgia Deliyannis [1,*,‡]

1 Department of Microbiology and Immunology, The University of Melbourne, The Peter Doherty Institute for Infection and Immunity, Melbourne, VIC 3000, Australia; pin.quah@unimelb.edu.au (P.S.Q.); vcorbin@unimelb.edu.au (V.D.A.C.); jessiejieyou@student.unimelb.edu.au (J.J.-Y.C.); chinnw@unimelb.edu.au (C.Y.W.); weiguang@unimelb.edu.au (W.Z.); preading@unimelb.edu.au (P.C.R.); davidcj@unimelb.edu.au (D.C.J.); lachlan.coin@unimelb.edu.au (L.J.M.C.)
2 Department of Infectious Diseases, The University of Melbourne, The Peter Doherty Institute for Infection and Immunity, Melbourne, VIC 3000, Australia; manht@unimelb.edu.au (B.M.T.); evincan@unimelb.edu.au (E.V.)
3 Asia-Pacific Centre for Animal Health, Melbourne Veterinary School, Faculty of Science, The University of Melbourne, Melbourne, VIC 3010, Australia; andres.diaz@unimelb.edu.au (A.D.-M.); carolah@unimelb.edu.au (C.A.H.)
4 Ian Holmes Imaging Centre, The University of Melbourne at BIO21, Parkville, VIC 3052, Australia; ehanssen@unimelb.edu.au (E.H.); zlatan@unimelb.edu.au (Z.T.)
5 Department of Biochemistry and Pharmacology, and ARC Training Centre for Cryo Electron Microscopy of Membrane Proteins, The University of Melbourne, Melbourne, VIC 3010, Australia
6 WHO Collaborating Centre for Reference and Research on Influenza, Victorian Infectious Diseases Reference Laboratory, The Peter Doherty Institute for Infection and Immunity, Melbourne, VIC 3000, Australia
7 Victorian Infectious Diseases Reference Laboratory, The Peter Doherty Institute for Infection and Immunity, Melbourne, VIC 3000, Australia
8 Curtin Medical School, Curtin University, Perth, WA 6102, Australia
* Correspondence: georgia.deliyannis@unimelb.edu.au
† These authors contributed equally to this work.
‡ These authors also contributed equally to this work.

check for updates

Citation: Quah, P.S.; Tran, B.M.; Corbin, V.D.A.; Chang, J.J.-Y.; Wong, C.Y.; Diaz-Méndez, A.; Hartley, C.A.; Zeng, W.; Hanssen, E.; Trifunovic, Z.; et al. Development of Matrix-Embedded Bovine Tracheal Organoids to Study the Innate Immune Response against Bovine Respiratory Disease. *Organoids* **2023**, 2, 82–101. https://doi.org/10.3390/organoids2020007

Academic Editor: Nicholas R. Forsyth

Received: 21 March 2023
Revised: 26 April 2023
Accepted: 7 May 2023
Published: 11 May 2023

Abstract: Bovine respiratory disease (BRD) is the leading cause of morbidity and mortality in feedlot cattle. Bovine herpesvirus-1 (BHV-1) is one of the main culprits of BRD; however, research on BHV-1 is hampered by the lack of suitable models for infection and drug testing. In this study, we established a novel bovine tracheal organoid culture grown in a basement membrane extract type 2 (BME2) matrix and compared it with the air–liquid interface (ALI) culture system. After differentiation, the matrix-embedded organoids developed beating cilia and demonstrated a transcriptomic profile similar to the ALI culture system. The matrix-embedded organoids were also highly susceptible to BHV-1 infection and immune stimulation by Pam_2Cys, an immunomodulator, which resulted in robust cytokine production and tracheal antimicrobial peptide mRNA upregulation. However, treatment of bovine tracheal organoid cultures with Pam_2Cys was not sufficient to inhibit viral infection or replication, suggesting a role of the non-epithelial cellular microenvironment in vivo.

Keywords: bovine respiratory disease; organoids; BHV-1; Pam_2Cys; BME2; air–liquid interface; single-cell RNA sequencing

1. Introduction

In 2022, more than 1 million Australian cattle were finished in feedlots, which is equivalent to more than 50% of the total beef production in the country [1]. Bovine

respiratory disease (BRD) is the major cause of clinical illness and death in feedlot cattle, threatening the beef industry in Australia and worldwide. BRD is a disease of the lower respiratory tract and is caused by a number of viral and bacterial pathogens which are collectively referred to as the bovine respiratory disease complex [2]. Respiratory viral infection is the key factor in predisposing cattle for the development of this disease complex. Viruses that play prominent roles in BRD include bovine herpesvirus-1 (BHV-1), bovine respiratory syncytial virus (BRSV), bovine parainfluenza-3 virus (BPIV-3) and bovine viral diarrhoea virus (BVDV). These viruses can cause direct damage to the mucociliary clearance mechanisms and the lung parenchyma, subsequently promoting migration of opportunistic bacteria from the upper respiratory tract and establishment of infection in the compromised lung [3]. In most cases of BRD, it is BHV-1 that is associated with the initiation of the respiratory disease complex because a high proportion of cattle (>80%) are seronegative for BHV-1 at feedlot entry and, therefore, susceptible to BHV-1 infection. In contrast, viral-specific antibodies against BRSV, BPIV-3 and BVDV are more prevalent in feeder cattle at entry [4].

BHV-1 is an alphaherpesvirus comprising a 136-kilobase double-stranded DNA genome, an icosadeltahedral capsid of approximately 100 nm and an envelope containing viral glycoprotein spikes on its surface [5]. It primarily infects epithelial cells of the respiratory mucosa and can establish latency following a primary infection [5,6]. When animals with latent infections are introduced into a feedlot, the high-stress environment due to transport, confined space and change of diet can result in reactivation, replication and subsequent transmission of BHV-1, resulting in an outbreak amongst the susceptible calves and initiation of the BRD complex [2,3]. There are vaccines available that are used in the control of BRD [7], but these vaccines offer only partial protection, usually because of immune evasion mechanisms by the pathogen [8]. Moreover, feedlot producers administer these vaccines to calves as they enter the feedlots, often in the face of an outbreak, which means that there is not sufficient time for calves to mount effective immune responses prior to exposure. Another major strategy for prevention and treatment of BRD involves extensive use of antibiotics [7]. Hence, there is a need to develop more effective therapeutic approaches to manage BRD and reduce reliance on antibiotics in the feedlot industry.

Innate immune responses act to limit pathogen replication and disease as early as within the first few hours of infection and well before the development of adaptive (immunoglobulin and cell-mediated) immune responses. Within the respiratory tract, toll-like-receptor (TLR)-mediated recognition of microbial pathogen-associated molecular patterns (PAMPs) expressed by inhaled pathogens initiates a complex and integrated signalling cascade that results in activation of innate immune defences [9]. Upon PAMP recognition, TLRs recruit adaptor proteins such as MyD88 and TRIF, which initiate signal transduction pathways that result in the activation of NF-kB and IRFs to regulate the expression of cytokines, chemokines and type 1 interferons (IFN) that ultimately protect the host from microbial infection [10]. Ten TLRs (TLR1 to TLR10) have been identified in cattle and all ten have been shown to be expressed in cultured bovine tracheal epithelial cells (bTEC), bovine tracheal mucosa and bovine lung [11].

Dipalmitoyl-S-glyceryl-cysteine (Pam_2Cys) is a synthetic analogue of the lipid component of macrophage-activating lipopeptide-2 (MALP2), which is found in numerous pathogens including *Mycoplasma fermentans*, and binds to TLR 2/6 heterodimer [12,13]. Intranasal administration of Pam_2Cys to mice stimulates production of inflammatory mediators including interleukin (IL)-6, IL-10, monocyte chemoattractant protein (MCP)-1, interferon (IFN)-γ and tumour necrosis factor (TNF)-α in bronchoalveolar lavage fluid, as well as recruitment of neutrophils, macrophages and IFN-γ^+ natural killer (NK) cells to the airways [14]. These effects were not observed in TLR2-deficient mice, confirming that the immunostimulatory effects of Pam_2Cys are dependent on TLR2 signalling [14]. Importantly, intranasal administration of Pam_2Cys to the upper respiratory tract of mice significantly reduced influenza viral load in the nasal epithelia and reduced viral progression to the lungs. This is attributed to the upregulation of cytokines (IL-6, TNFα, IL-1α and IL-1β)

and chemokines (CXCL1, CCL2, CCL3 and CCL4) in the nasal turbinates which recruit immune cells to the site of infection [15]. Bone marrow chimera experiments demonstrated that both radioresistant epithelial cells and non-radioresistant immune cells played a role in the protection conferred by Pam_2Cys treatment [15]. In vitro experiments using murine lung epithelial cells (LA-4) further showed that pre-treatment with Pam_2Cys restricted viral replication following subsequent challenge with influenza virus [15]. However, the antiviral effect of Pam_2Cys on bovine airway epithelium is not well understood.

Models for BHV-1 infection have been developed using conventional in vitro 2D monolayer continuous cell lines [16–18], or primary airway epithelial cell cultures [19]. A more complex model involves organ explant culture derived from precision-cut lung slices [17]. Recently, there has been advancement in using in vitro organoid culture systems as models for studying respiratory viral infections such as SARS-CoV-2 [20]. Among models for BHV-1 infection in bovines, there are air–liquid interface (ALI) cultures [17], bovine corneal cultures [21] and primary cultures derived from respiratory explants [22]. ALI culture appears to be one of the best models for its capabilities to recapitulate the diverse and complex composition of mucociliary differentiation while retaining the characteristics of the primary tissue [23,24]. However, there is no report on culturing matrix-embedded bovine airway organoids, which is a very popular method in cell biology and cancer research because it enables expansion of the organoids [25]. Matrix-embedded organoids offer several advantages: the basement matrix acts as a scaffold that helps stem cell proliferation in 3D structures which better mimics the complex features of the target organ in terms of histology, metabolism and functionalities. This is because the architecture, topographical cue and elastic properties of extracellular-matrix-like material provides external and intrinsic mechanical forces that guide biochemical signalling in cell proliferation and differentiation [26,27]. In this study, we generated bovine tracheal epithelial organoids in a basement membrane extract matrix and modelled BHV-1 infection. The culture was then used to evaluate the inhibitory effect of Pam_2Cys treatment on viral infection.

2. Materials and Methods

2.1. Synthesis of Pam_2Cys

The synthesis of Pam_2Cys has been previously described [14]. The final, totally synthetic product contained no detectable lipopolysaccharide (<0.05 endotoxin units/mL) as determined using the Limulus amebocyte lysate assay (Lonza, Basel, Switzerland). The quality of synthesised Pam_2Cys was confirmed by Agilent 1100 series capillary LC system in line with an Agilent 1100 series LC/MSD ion-trap mass spectrometer (Santa Clara, CA, USA). Newly synthesised Pam_2Cys' stimulatory effect on TLR2 signalling was confirmed by HEK-Blue hTLR2 assay (InvivoGen, San Diego, CA, USA) performed according to the manufacturer's instructions.

2.2. Isolation of Bovine Tracheal Epithelial Cells

Two bovine tracheas were obtained from an abattoir from beef cattle that had been slaughtered for domestic human consumption. The tracheas were collected from discarded offal, and from the size of the tracheas, we estimated that the animals were approximately 12 months of age. The tracheas were processed as previously described [28,29]. Briefly, the tracheas were cut into three sections before dissecting the mucosal tissue from the cartilage. Mucosal tissue sections were washed three times with ice-cold washing solution to remove blood cells, mucus and debris. The washing solution consisted of calcium- and magnesium-free phosphate-buffered saline ($PBS^{=}$) supplemented with 1000 U/mL penicillin/streptomycin (Thermo Fisher Scientific, Waltham, MA, USA), 0.5 mg/mL of gentamicin (Pfizer, New York, NY, USA), 10 µg/mL amphotericin B (Sigma-Aldrich, St. Louis, MO, USA), 8 µg/mL of cefoperazone (Sigma-Aldrich, St. Louis, MO, USA) and 4 µg/mL of teicoplanin (Sandoz, Basel, Switzerland). The tissue sections were then submerged in washing solution containing 0.1% (*w/v*) protease (Pronase from *Streptomyces griseus*, Roche, Basel, Switzerland) overnight at 4 °C. After at least twelve hours of incubation, 10% (*v/v*)

heat-inactivated foetal bovine serum (FBS) was added to neutralise enzymatic digestion. The mucosa was washed three times with ice-cold washing solution and mucosal scrapings of the tracheal cells were collected into a tube containing minimum essential media and 10% (*v/v*) FBS. The tracheal epithelial cells were mechanically separated using a pipette and pelleted by centrifugation at 500× *g*, 4 °C for 10 min. Recovered epithelial cells were stored in liquid nitrogen at a density of 1×10^7 cells/cryovial for Animal 1 and Animal 2.

2.3. Culture of Bovine Tracheal Epithelial Monolayers

Bovine tracheal epithelial cell monolayers were grown as previously reported in [11,30] with modification. In our study, 24-well culture plates were pre-coated with 300 µL of 0.01% (*w/v*) collagen type I solution from rat tail (Sigma-Aldrich, St. Louis, MO, USA) in sterile $PBS^=$ and incubated overnight at 4 °C. After thawing and washing, 0.5×10^6 cells of primary bovine tracheal cells were cultured on the plate with 500 µL of medium comprising Advanced DMEM/F-12 (Thermo Fisher Scientific, Waltham, MA, USA), 1× GlutaMAX (Thermo Fisher Scientific, Waltham, MA, USA), 1000 U/mL penicillin/streptomycin (Thermo Fisher Scientific, Waltham, MA, USA), 24 µg/mL of gentamicin (Pfizer, New York, NY, USA), 0.25 µg/mL of amphotericin B (Thermo Fisher Scientific, Waltham, MA, USA), insulin–transferrin–sodium selenite (ITS) liquid media supplement (Sigma-Aldrich, St. Louis, MO, USA), 25 ng/mL of epidermal growth factor (EGF) from murine submaxillary gland (Sigma-Aldrich, St. Louis, MO, USA) and 25 µg/mL of bovine pituitary extract (PGE) (Sigma-Aldrich, St. Louis, MO, USA). The cell culture medium was changed by removing 500 µL of spent medium and replacing with equal volume of fresh pre-warmed medium. Media change was performed every two to three days until monolayers were 60–70% confluent.

2.4. Expansion of Basal Progenitors in PneumaCult ExPlus

T-25 flasks were coated overnight with PureCol-S collagen type I (Advanced BioMatrix, Carlsbad, CA, USA) diluted to 30 µg/mL in $PBS^=$. Bovine tracheal epithelial cells stored in liquid nitrogen were thawed, washed, and resuspended in PneumaCult ExPlus medium (STEMCELL Technologies, Vancouver, BC, Canada) with antibiotics (1000 U/mL penicillin/streptomycin, 24 µg/mL of gentamicin, 0.25 µg/mL of amphotericin B) at 2.5×10^5 viable cells/mL and transferred to pre-coated flasks. Flasks were incubated at 37 °C, 5% CO_2. The medium was replaced with fresh pre-warmed medium on day 3 and day 5. Cells were harvested when they reached 60–80% confluency on day 7. Aliquots of cells were used to set up organoid cultures or were cryopreserved.

2.5. Culture of Matrix-Embedded Bovine Tracheal Organoids

Cell pellets (ExPlus-expanded cells) were resuspended in ice cold Cultrex Reduced Growth Factor Basement Membrane Extract, Type 2 (BME2) (R&D Systems, Minneapolis, MN, USA) at 10,000 cells/50 µL and plated on the pre-warmed plate. After the matrix was set, 500 µL of PneumaCult Airway Organoid Seeding Medium (AOSM) (STEMCELL Technologies, Vancouver, BC, Canada) with 50 µg/mL of ampicillin (Sigma-Aldrich, St. Louis, MO, USA) was then added to the each well. Samples were incubated at 37 °C, 5% CO_2 for 7 days. Media change was performed every 2–3 days. After 7 days, the cell culture medium was switched from AOSM to PneumaCult Airway Organoid Differentiation Medium (AODM) (STEMCELL Technologies, Vancouver, BC, Canada) with 50 µg/mL of ampicillin (Sigma-Aldrich, St. Louis, MO, USA). Organoids were cultured in AODM for 14–21 days. Media change was performed every 2–3 days by replacing the spent medium with 500 µL of pre-warmed, fresh AODM.

2.6. Culture of Bovine Tracheal Epithelial Cells at an Air–Liquid Interface (ALI)

Cryopreserved PneumaCult ExPlus-expanded cells were thawed and seeded onto 6.5 mm Transwell inserts with 0.4 µm pore diameter and 4×10^6 pores/cm^2 (Corning, Kennebunk, ME, USA) pre-coated with PureCol-S (Advanced BioMatrix, Carlsbad, CA, USA)

at a cell density of 2×10^5 cells/insert. PneumaCult-ExPlus (STEMCELL Technologies, Vancouver, BC, Canada) with antibiotics (1000 U/mL penicillin/streptomycin, 24 µg/mL of gentamicin, 0.25 µg/mL of amphotericin B) were added to the apical (150 µL) and basal (750 µL) compartments. Cells were incubated at 37 °C, 5% CO_2. On day 4, the apical and basal media were removed and replenished with fresh pre-warmed PneumaCult-ExPlus medium with antibiotics. On day 7, the PneumaCult-ExPlus medium was switched to PneumaCultALI medium with 50 µg/mL of ampicillin for both apical and basal compartments (STEMCELL Technologies, Vancouver, BC, Canada). After 2 days, ALI was initiated by removing the medium from the apical compartment and only adding fresh PneumaCult ALI medium with ampicillin to the basal compartment. The basal medium was replaced every 2–3 days for 9 days.

2.7. Live Cell Imaging

Brightfield images and movies of cilia beating in the cultures were captured on an Olympus CKX41 microscope running CellSens software using an SC30 camera.

2.8. Immunofluorescence and Confocal Microscopy

The BME2 samples were washed thrice with PBS containing calcium and magnesium (PBS^{++}) at room temperature and fixed with 4% paraformaldehyde (Electron Microscopy Sciences, Hatfield, PA, USA) for 1 h at room temperature (RT). The fixative was aspirated and neutralised with 100 mM glycine in PBS^{++} for 10 min at RT. BME2 was dissolved by adding ice-cold PBS^{++}, mixed gently by pipetting and centrifuged for 5 min at 300× *g*, 4 °C. Cell pellets were resuspended in ice-cold PBS^{++} and centrifuged as before. The organoids were transferred to a Tissue-Tek® biopsy cryomold (Sakura Finetek, Torrance, CA, USA) and filled with Tissue-Tek® O.C.T. compound (Sakura Finetek, Torrance, CA, USA). The embedded organoids were snap-frozen with liquid nitrogen and cryosectioned at 10 µm, transferred to glass slides and air-dried overnight. For immunofluorescence staining, a circle was drawn around the sample on a glass slide with a Dako hydrophobic pen (Agilent Technologies, Santa Clara, CA, USA). The cryosections were then submerged in PBS^{++} for 10 min in a Coplin jar to remove the O.C.T. and to rehydrate the tissue. From this step onwards, the slides were kept moist in a humidity chamber. Permeabilisation buffer (PB, 0.5% Triton-X in PBS^{++}) was added to the samples and at 4 °C for 30 min. The PB was washed off with 3 washes of PBS^{++}, 5 min each. This was followed by incubating the samples for 90 min at 4 °C in immunofluorescence buffer (IF, PBS^{++} with 0.1% bovine serum albumin, 0.2% Triton, 0.05% Tween 20) containing 10% normal goat serum (BB, block buffer). At the end of incubation, the BB was removed and mouse monoclonal anti-acetylated tubulin (clone 6-11B-1) (Sigma-Aldrich, St. Louis, MO, USA) or mouse IgG isotype control (Thermo Fisher Scientific, Waltham, MA, USA), both diluted in BB, were added. Following 48 h incubation at 4 °C, the primary antibody was washed off with IF buffer, three times, 5 min each. Goat anti-mouse Alexa Fluor™ 647 (Thermo Fisher Scientific, Waltham, MA, USA) and Hoechst (Thermo Fisher Scientific, USA), diluted in BB, were added and slides were incubated for 3 h, at RT. Secondary antibody was washed off with IF buffer, five times, 5 min each. Tissue sections were incubated with Phalloidin Fluor™ 555 for 30 min and washed once with PBS^{++}. This was followed by incubation with DAPI for 20 min, washing once with PBS^{++} and mounting in FluoroSave Reagent (EMD Millipore, Billerica, MA, USA) on glass slide; coverslips were sealed with nail polish. The ALI samples were fixed and stained as described elsewhere [31], using the same antibodies as the BME2 samples. The confocal microscopy imaging was acquired on the Zeiss LSM 780 system. The acquired Z-sections were stacked and processed using ImageJ software.

2.9. Single-Cell RNA Sequencing

Undifferentiated PneumaCult ExPlus-expanded cells, organoids grown in BME2, organoids grown at ALI and organoids grown at ALI which had been treated with Pam_2Cys were subjected to transcriptomic sequencing. Single-cell barcoded cDNA and Illumina

libraries were prepared from these samples using the Cell Fixation Kit (Parse Biosciences, Seattle, WA, USA) and Evercode Whole Transcriptome Mini Kit (Parse Biosciences, Seattle, WA, USA) according to manufacturer's instructions. For BME2 organoids, cell pellets from three wells were pooled. For organoids grown at ALI, the filters were excised from three Transwell inserts per condition and pooled. Cells were dissociated from BME2 organoids and ALI by incubating in TripLE™ Express Enzyme (Thermo Fisher Scientific, Waltham, MA, USA).

For the preparation of libraries for Illumina sequencing, 100 ng of each sub-library was subjected to fragmentation, size selection using AMPure XP beads, amplification and ligation of the second Illumina adaptor ligation. The cDNA fragments were cleaned up again with AMPure XP beads post-ligation and amplified to add the fourth barcode and the P5 and P7 adaptors. Two different index primers were used in each sub-library. A final size selection using AMPure XP beads was carried out before checking the cDNA yield and quality as above. Sequencing was performed by the Australian Genome Research Facility (AGRF Ltd., Melbourne, VIC, Australia) using Illumina NovaSeq 6000. The sequence reads were analysed according to AGRF quality control measures.

2.10. Bioinformatics Analysis

The two sub-libraries were sequenced separately, resulting in two batches of sequencing data. Each batch was first processed using Parse BioSciences' pipeline split-pipe, which identifies barcodes, aligns reads and creates a cell-by-gene count matrix which can be used to perform PCA and clustering of cells. The count matrices from the two batches were then combined using split-pipe 'comb' mode. The resulting count matrix was used as an input into Seurat for further analysis. Cells from untreated ALI and BME2 were compared to undifferentiated control cells by performing PCA followed by UMAP using the first 30 dimensions for visualisation.

To identify the cell types present in each sample, the cells from treated ALI and untreated ALI and BME2 were first integrated with each other by removing sample-specific variances in the cell-by-gene count matrix using Seurat 'IntegrateData' function. The cells were then clustered by using a combination of PCA and KNN clustering on the first 30 dimensions with a resolution of 0.3. A UMAP dimensional reduction was then used for visualisation.

While there are no established marker genes for bovine tracheal cells, marker genes for various human tracheal cells have been identified. Using the existing literature [32–34], a list of marker genes for each human tracheal cell type was compiled. That list was then converted for bovine by using bovine homologues to the human genes. The homologues were identified using BovineMine. The clusters identified by Seurat were mapped to tracheal cell types by comparing the differentially expressed genes specific to each cluster to the bovine cell type markers. For this, the genes identified in the publications were considered for assigning the cell types [32–34]. Next, if clusters were unable to be assigned, a secondary assignment with the top 10 genes sorted by descending z-scores on the human airway atlas [32] was carried out. Differential expression analysis for each cluster against all other clusters was carried out by the Seurat 'FindAllMarkers' function using Wilcoxon's test of ranks and default parameters.

2.11. Measurement of Cytokine Production

To investigate the effect of Pam_2Cys on cytokine production and BHV-1 infection, monolayers and BME2 organoids were treated in duplicate or triplicate with 500 µL of cell culture media containing 1, 5 or 10 nmol/mL of Pam_2Cys and incubated at 37 °C, 5% CO_2. Supernatants were collected after 24 h. Supernatants were used at neat to measure IL-6 levels and diluted with diluent at a ratio of 1:5 to measure IL-8 levels. IL-6 levels were measured using the Bovine IL-6 DuoSet ELISA kit (R&D Systems, Minneapolis, MN, USA) according to manufacturer's specifications unless otherwise specified. IL-8 levels were measured using the Bovine IL-8 Do-It-Yourself ELISA kit (Kingfisher Biotech, St Paul, MN,

USA). Optical density was determined using CLARIOstar Plus plate reader (BMG Labtech, Ortenberg, Germany) set at 450 nm and 570 nm. The readings at 570 nm were subtracted from the readings at 450 nm for wavelength correction. Data were analysed using the MARS Data Analysis Software (BMG Labtech, Ortenberg, Germany). Four-parameter logistic regression was used to fit symmetrical data whereas five-parameter logistic regression was used to fit asymmetrical data.

2.12. Reverse Transcription Quantitative PCR (RT-qPCR)

RNA was extracted from 10 nmol/mL-Pam_2Cys-treated and untreated BME2 organoids at 6 h and 24 h post-induction, following RNeasy kit (Qiagen, Hilden, North Rhine-Westphalia, Germany) manufacturer's instructions. Complementary DNA (cDNA) was synthesised using 100 ng of RNA and the Omniscript Reverse Transcription Kit (Qiagen, Hilden, North Rhine-Westphalia, Germany). Each sample contained 5.35 µL of the Mastermix with or without reverse transcriptase and 14.65 µL of RNA templates diluted in diethyl-pyrocarbonate (DPEC)-treated water. cDNAs were diluted 1:10 and RT-qPCRs were carried out in a final volume of 10 µL containing (i) Sso Advanced universal SYBR Green Supermix (Bio-Rad, Hercules, CA, USA), (ii) primers, (iii) cDNA and (iv) water. The primers have been published by Berghuis et al. [11] and are listed in Table 1. RT-qPCR assays were performed using the Quantstudio™ 7 Flex thermocycler. The fold change was calculated as $2^{-\Delta\Delta Ct}$. $\Delta\Delta Ct$ = (Ct *TAP* − Ct *GAPDH*) of each time point − (Ct *TAP* − Ct *GAPDH*) of the untreated organoids as previously described [35].

Table 1. Primer sequences for RT-qPCR.

Gene	Primer	Sequence
GAPDH	Forward	5′-GGCGTGAACCACGAGAAGTATAA-3′
	Reverse	5′-CCCTCCACGATGCCAAAGT-3′
TAP	Forward	5′-TCTTCCTGGTCCTGTCTGCT-3′
	Reverse	5′-GCTGTGTCTTGGCCTTCTTT-3′

2.13. Preparation of BHV-1 Stocks

The vaccine strain of BHV-1 was propagated from Rhinogard Intranasal Vaccine, (B)BHV4816/02, APVMA Number 65951/57657 (Zoetis Australia Pty Ltd., Rhodes, NSW, Australia). BHV-1 strain 4663 (field strain) was isolated from the nasal cavity of a calf as we previously described [36]. The viruses were propagated in Madin Darby bovine kidney (MDBK) cells. Specifically, MDBK cells were grown to 70% confluency in T-175 flasks using 40 mL of RPMI-1640 (Thermo Fisher Scientific, Waltham, MA, USA) supplemented with 5% (*v/v*) heat-inactivated FBS, GlutaMAX™ (Thermo Fisher Scientific, Waltham, MA, USA), 1 mM sodium pyruvate, 1000 U/mL penicillin–streptomycin and 24 µg/mL gentamicin (now referred to as RP5 medium). An amount of 1 mL of virus stock was diluted to a total volume of 10 mL with RP1 medium, which has the same composition as RP5 except that it contained 1% (*v/v*) FBS. RP5 was removed and the diluted stock was added to the cells. The flask was incubated at 37 °C, 5% CO_2. After 1 h, 10 mL RP1 was added to prevent the cells from drying out. The flask was returned to the 37 °C incubator for another 30 min before adding an additional 20 mL of RP1. Supernatant (passage 1) was harvested after 3 days, when >90% of the cells had detached from the flask. Aliquots of passage 1 were stored at –80 °C. Passage 1 was thawed, and 1.6 mL was diluted to 20 mL with RP1 and added to a new T-175 flask with MDBK cells. The flask was incubated at 37 °C, 5% CO_2. After 45 min, 20 mL RP1 was added to the flask which was then returned to the 37 °C incubator with 5% CO_2. Supernatant (passage 2) was harvested 2–3 days later (>90% of the cells had detached from the flask) and centrifuged at 800× *g*, room temperature. Aliquots were made and stored at −80 °C. Passage 2 was used for all infection assays in this paper.

2.14. Infection of Bovine Tracheal Monolayers and Matrix-Embedded Organoids with BHV-1

To infect monolayers with BHV-1, the virus was added at a multiplicity of infection (MOI) of 0.01 in 200 µL of inoculum to each monolayer. After virus adsorption for 1 h at 37 °C with 5% CO_2, the inoculum was removed and the monolayers washed three times with cell culture medium (without ITS, EGF and PGE) three times. The final wash was collected to determine the time zero (T0)/background viral tires. An amount of 1 mL of pre-warmed complete cell culture media was added to the monolayers which were then incubated at 37 °C with 5% CO_2. An amount of 500 µL of cell culture supernatant was collected after 24 h, and the final 500 µL of supernatant was harvested after 48 h. All supernatants were stored at –80 °C until used.

To infect BME2-embedded organoids, 500 µL of BHV-1 at 10^4 PFU/mL was added to each well and incubated for 1 h at 37 °C with 5% CO_2. After virus adsorption, the inoculum was removed and 500 µL of pre-warmed RPMI (Thermo Fisher Scientific, Waltham, MA, USA) was added to the BME2-embeded organoids. The samples were placed in the 37 °C incubator with 5% CO_2 for 10 min; this step was performed three times. The final wash was collected to determine the time zero (T0)/background viral tires. An amount of 1 mL of pre-warmed AODM was added to each well. Samples were incubated at 37 °C with 5% CO_2. An amount of 500 µL of cell culture supernatant was collected after 24 h, and the final 500 µL of supernatant was harvested after 48 h. All supernatants were stored at −80 °C until used.

2.15. Determination of Viral Titres

Plaque assay on confluent monolayers of MDBK cells was used to determine the titres of infectious virus. Six-well tissue culture plates were seeded with 1.2×10^6 MDBK cells per well in 3 mL of RP5. After overnight incubation at 37 °C in 5% CO_2, confluent monolayers were washed with RPMI containing antibiotics (1000 U/mL penicillin–streptomycin and 24 µg/mL gentamicin). Test supernatants from the 24 h and 48 h timepoints were serially diluted in RPMI (Thermo Fisher Scientific, Waltham, MA, USA) containing antibiotics; T0 supernatants were used undiluted. An amount of 125 µL of these supernatants were added to wells of MDBK monolayers and incubated for 45 min at 37 °C 5% CO_2. Monolayers were then overlaid with 3 mL of Leibovitz L15 medium (pH 6.8) (Thermo Fisher Scientific, Waltham, MA, USA) containing 0.9% (*w/v*) agarose (Sigma-Aldrich, St. Louis, MO, USA) and antibiotics. All assays were carried out in duplicate. Plates were incubated for 7 days at 37 °C in 5% CO_2. Two mL of 10% neutral buffered formalin solution (Sigma-Aldrich, St. Louis, MO, USA) was added directly to the agar in a fume hood and incubated for 40 min at room temperature. The 10% formalin was discarded, and the agar was removed. An amount of 1 mL of 0.1% toluidine blue solution (Hurstchem, Forrestdale, WA, Australia) was added to each well and incubated for 30 min with gentle shaking on a plate shaker. Toluidine blue solution was removed, and the monolayers were washed gently under running tap water. Plates were dried overnight before plaque forming units (PFUs) were counted.

2.16. Transmission Electron Microscopy

Organoids were fixed in 2.5% glutaraldehyde (Electron Microscopy Sciences, Hatfield, PA, USA) at 4 °C overnight, washed in 0.175 M sodium cacodylate before being post-fixed with reduced osmium tetroxide and further processed as described previously [37]. Ultrathin sections (70 nm) were observed on a Tecnai F30 transmission electron microscope (FEI, Eindhoven, The Netherlands) at the Ian Holmes Imaging Centre, Bio21, University of Melbourne. Micrographs were taken using an FEI CETA CMOS detector.

2.17. Statistical Analysis

All statistical analyses were performed using GraphPad Prism 9 (GraphPad Software, San Diego, CA, USA). Prior to analysis, each data set was tested for a normal distribution using the Shapiro–Wilk test. Welch's or Brown–Forsythe tests were used to test for unequal

variances. When the data were collected for one independent variable, one-way ANOVA was used for comparisons between more than two groups of normally distributed data. ANOVA was followed by Dunnett's (for data with equal variance) or Dunnett's T3 (for data with unequal variance) multiple comparison tests. Non-normally distributed data were analysed with the Kruskal–Wallis test with Dunn's post hoc test for comparisons between more than two groups of data. When the data were collected for two independent variables, significance was determined with two-way ANOVA, followed by Dunnett's multiple comparisons post hoc test. The results were considered statistically significant if p-values < 0.05.

3. Results

3.1. Establishment and Characterisation of Bovine Tracheal Epithelial Organoids

To evaluate bovine tracheal organoid culture as a model for infectious disease, bovine basal progenitor cells were collected, and organoid cultures were established and infected. Notably, thawed basal progenitor cells seeded into tissue culture flasks initially formed small patches on the tissue culture surface. These patches gradually expanded and reached 60–80% confluency after 7 days. On day 7, cells exhibited a cobble-stone cuboidal morphology with epithelial characteristics (Figure 1A). When re-seeded into BME2 matrix culture, each small group of cells formed spherical organoid structures and continued expanding. Switching to AODM slowed down the expansion and stimulated the differentiation process, which was characterised by morphological folding of the organoids, nodule development and branching out of short strands of cells on the outer layers (Figure 1A). At the end of the differentiation process, these organoids also demonstrated the formation of beating cilia (Videos S1 and S2). Cilia formation was confirmed by staining for acetylated tubulin (Figure 1B) and electron microscopy (Figure 1C). In a similar manner, bovine cells expanded on Transwell filters started to differentiate under an ALI culture condition. The differentiation features included a thickening of the cell layer and the formation of a complex morphology with a clear apical–basal polarity. At the end of the differentiation period, secreted mucus and beating cilia were widely observed across the apical side of the culture (Figure 1B).

Single-cell transcriptomic sequencing analysis of tracheal organoids demonstrated that the differentiation process resulted in profound changes in transcriptomic profiles when undifferentiated and differentiated cells were compared (Figure 2A). Interestingly, whilst there was a clear segregation of ALI and BME2 organoids, they showed a similarity of their cell type composition which could be grouped into 10 clusters (Figure 2B and Table 2), each having a distinct gene signature profile. In general, the 10 clusters can be categorised into 3 groups: the basal cell group (clusters 1–6), secretory cell group (clusters 7 and 8) and ciliated cell group (clusters 9 and 10). For the basal cell group, ALI organoid cultures possessed remarkably higher proportions of cells in clusters 2, 3 and 4 than BME2 organoid cultures. Conversely, BME2 organoids showed a greater presence of ciliated cells compared to ALI organoid culture. Interestingly, this population of ciliated cells appears to be the outlier in the culture (indicated by arrow on Figure 2A). We noted that the number of single cells in clusters 9 and 10 were small, which might be caused by biological variation or sample preparation. Furthermore, despite mucus being observed visually via microscopy, high expressions of secretory mucins (e.g., *MUC5AC* and *MUC5B*) or secretoglobins (e.g., *SCGB1A1*) were not found in these clusters.

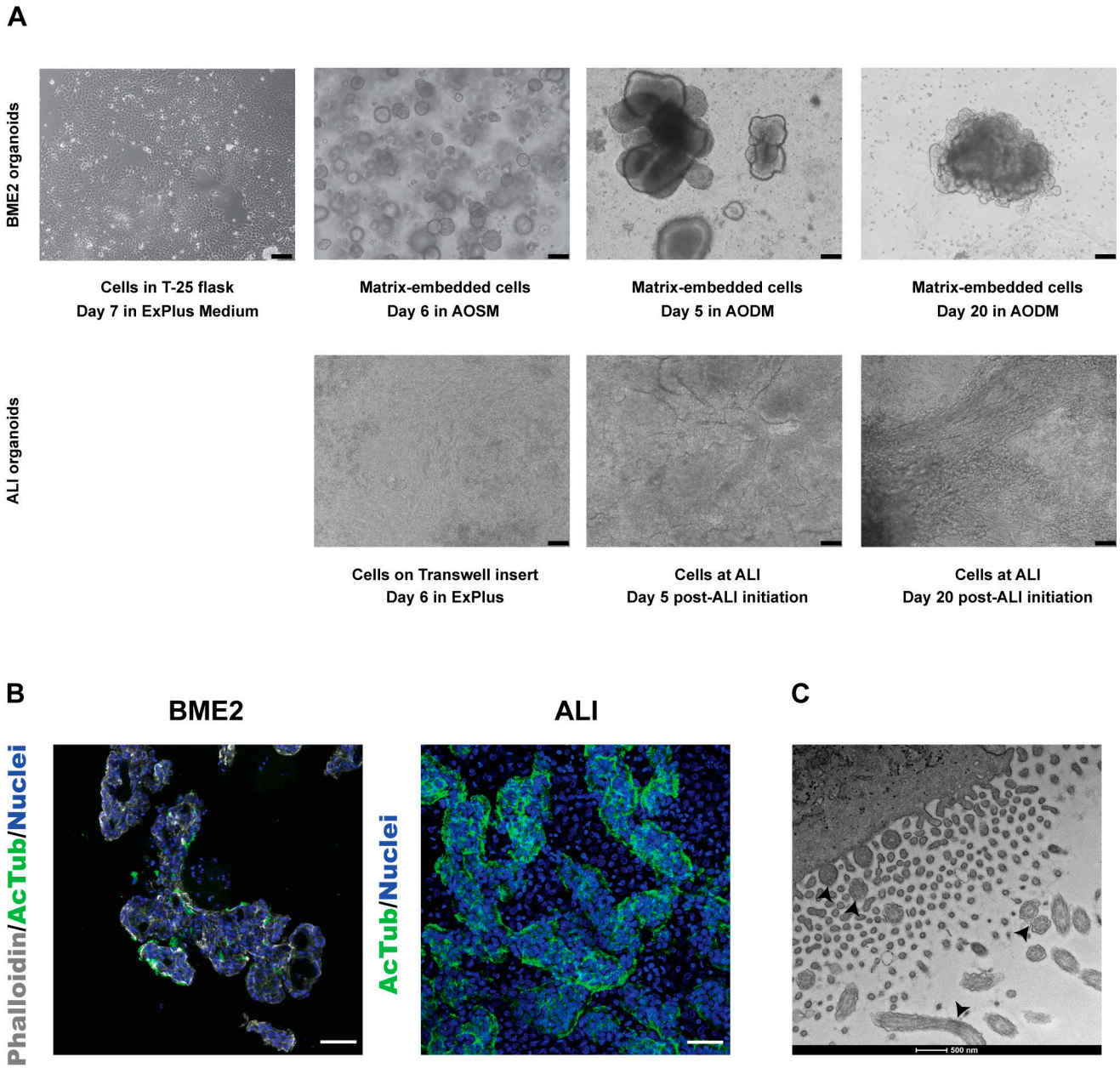

Figure 1. Establishment of bovine tracheal organoid cultures. (**A**) Bright-field images of BME2-matrix-embedded and ALI cultures during expansion and differentiation process at the indicated times. Scale bar is 100 µm. (**B**) Immunofluorescent confocal microscopy staining for α-tubulin (AcTub, green), F-actin (phalloidin, grey-white) and DAPI (nuclei, blue). Scale bar is 50 µm. (**C**) TEM imaging of bovine tracheal organoids grown in BME2 matrix; arrows indicate cilia.

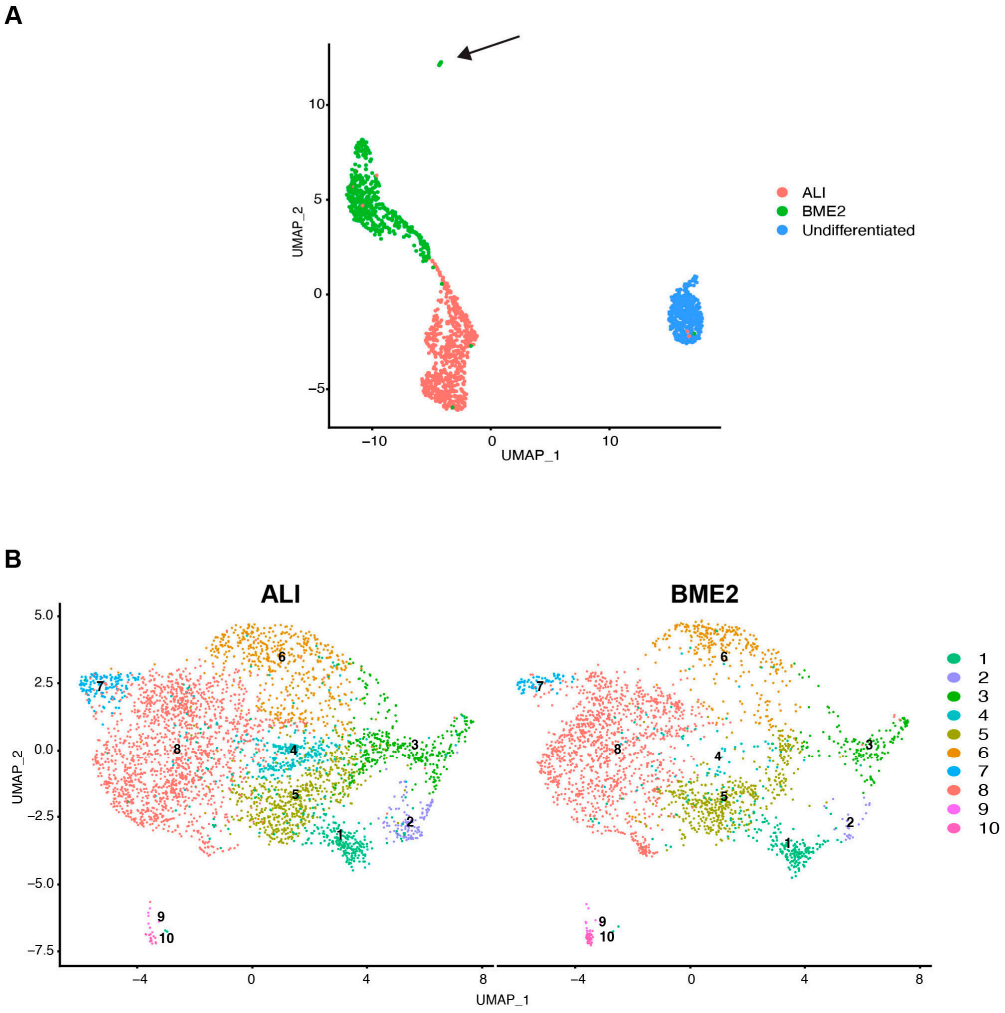

Figure 2. Single-cell transcriptomic analysis identifying bovine organoid cell types. (**A**) UMAP plot showing clustering of undifferentiated bovine tracheal cells, and organoids grown in air–liquid interface (ALI) and type 2 basement membrane extract (BME2) cultures. Arrow points to outliner population of cells from BME2 culture. (**B**) UMAP plots showing cell type classification of ALI and BME2 organoids, as determined by Seurat analysis. UMAP, uniform manifold approximation and projection.

Table 2. The expression of genes associated with differentiation markers in bovine airway epithelial cells. Genes in blue are markers derived from top 10 genes sorted by z-score in the human airway atlas by Deprez et al. [32].

Cluster	Cell Type	Marker Genes
1	Cycling basal	*MKI67*
	Neuroendocrine	*SYT1*
2	Basal	*TP63*, *KRT5*, *S100A2*,*PTMA*
	Ciliated	*TUBB4B*
	Cycling basal	*MKI67*, *HMGB2*
	Deuterosomal	*PLK4*
	Suprabasal	*KRT5*
	Neuroendocrine	*SYT1*

Table 2. *Cont.*

Cluster	Cell Type	Marker Genes
3	Basal	*TP63*, *KRT5*, *DAPL1*, *PTMA*,*S100A2*
	Cycling basal	*MT2A*,*GAPDH*,*PTTG1*
	Suprabasal	*KRT5*
	Neuroendocrine	*SYT1*
4	Basal	*KRT5*
	Suprabasal	*KRT5*
	Mucous	*AGR2*
5	Basal	*S100A2*, *PTMA*
	Mucous	*AGR2*
	Neuroendocrine	*SYT1*
6	Basal	*KRT15*
	Ionocytes	*CFTR*
	Cycling basal	*GAPDH*
	Suprabasal	*KRT4*, *KRT15*, *KRT19*
7	Secretory	*CXCL17*
	Basal	*KRT15*
	Suprabasal	*KRT4*, *KRT15*
	Serous	*TCN1*
	Mucous	*GOLM1*
8	Secretory	*CXCL17*,*TFF3*
	Ionocytes	*CFTR*
	Suprabasal	*KRT4*, *KRT15*, *TXN*
	Serous	*LTF*, *TCN1*
	Mucous	*GOLM1*,*TFF3*
9	Ciliated	*CCDC113*, *FOXJ1*, *MLF1*, *TPPP3*
	Secretory	*MSMB*
	Deuterosomal	*CDC20B*, *PLK4*, *DEUP1*, *KIF9*
	Serous	*LTF*
10	Ciliated	*CCDC113*, *FOXJ1*, *MLF1*, *TPPP3*, *TUBB4B*
	Secretory	*CYP2F1*
	Tuft/Brush	*GNAT3*
	Cycling basal	*PTTG1*
	Deuterosomal	*CDC20B*, *PLK4*, *DEUP1*, *KIF9*

3.2. Infection of Bovine Tracheal Epithelial Organoid with BHV-1

To evaluate the infectivity of BHV-1 on organoid cultures, we used both the vaccine strain, which is an attenuated form of BHV-1 generated by numerous passages through cell culture, and a field isolate representing the wild-type version of the virus. Firstly, we tested and showed a robust infection by both BHV-1 strains on bovine tracheal organoids expanded in 2D monolayer culture for both Animal 1 and Animal 2 (Figure 3A). The vaccine strain showed a slightly higher viral titre in plaque assay compared to the field isolate; however, this could be due to the adaptation of the vaccine strain to tissue culture, given it has been maintained in culture through passage since it was first isolated in

1964 [38]. Previous study showed that differentiated bovine bronchial epithelial cells grown in ALI culture were susceptible to BHV-1 infection from the basal side [17]. In this study, we investigated the infection of BHV-1 on our newly established BME2 bovine tracheal organoid model. After 48 h post-infection, both strains demonstrated strong infectivity in the 3D-matrix-embedded organoids (Figure 3B). The result was consistent between Animal 1 and Animal 2.

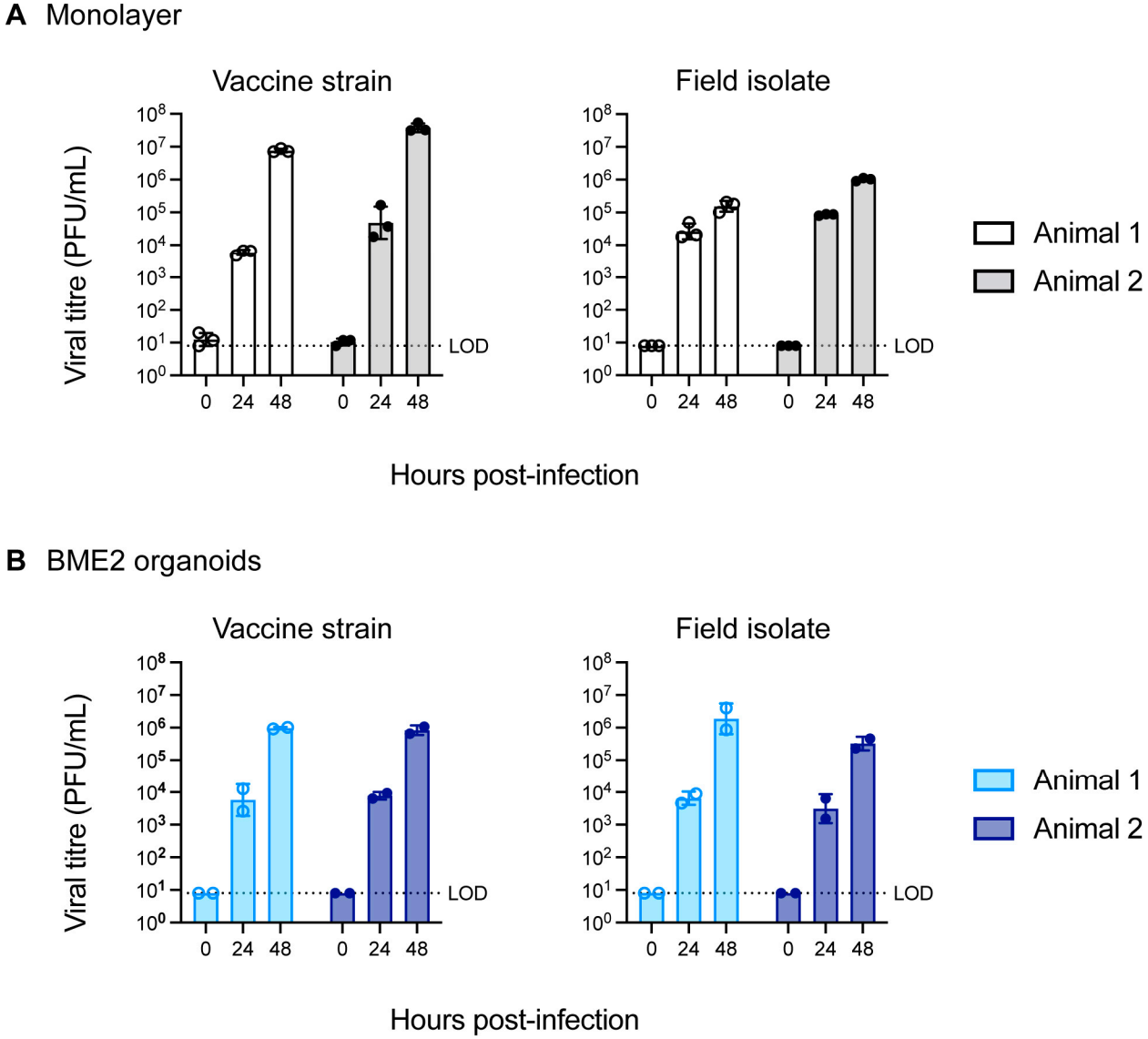

Figure 3. Replication of BHV-1 vaccine strain and field isolate in bovine tracheal monolayers as compared to 3D organoids. (**A**) Tracheal cells from two calves were grown into undifferentiated cell monolayers, which were inoculated with BHV-1 vaccine strain (left) and field isolate (right) at an MOI of 0.01. (**B**) Tracheal cells from the same animals were also grown into differentiated cultures of 3D organoids in BME2 matrix. Similarly, the 3D organoid cultures were infected with BHV-1 vaccine strain (**left**) and field isolate (**right**) at a viral titre of 10^4 PFU/mL. Supernatants were harvested at the indicated times to determine the viral titre by performing the plaque assay. For each animal, data represent the geometric mean values of two or three technical replicates. Error bars indicate the geometric standard deviation. BHV-1, bovine herpesvirus-1; LOD, limit of detection.

3.3. Innate Immune Response to TLR2 Ligand Pam_2Cys in Bovine Tracheal Cell Monolayer and BME2 Organoid

TLR2 activation by Pam_2Cys results in the production of cytokines and chemokines such as IL-6 and IL-8 in the murine respiratory tract [15]. IL-6 is a pleiotropic cytokine with a wide range of functions during viral infections, particularly in immune regulation, inflammation and tissue remodelling [39]. IL-8 is a chemokine which plays key roles in recruiting neutrophils and other immune cells to the site of infection [40]. To understand the effect of Pam_2Cys in stimulating the innate response in bovine tracheal epithelial cells, we first stimulated the monolayers grown from Animal 1 and Animal 2 with Pam_2Cys for 24 h, and then examined IL-6 and IL-8 levels in the supernatants by ELISA. Exposure of the monolayers from Animal 1 to an increasing dosage of Pam_2Cys (1, 5 and 10 nmol/mL) induced the production of IL-6 and IL-8 in a dose-dependent manner (Figure 4A,B). In our study, 1 nmol/mL of Pam_2Cys was sufficient to cause a significant increase in IL-6 and IL-8 levels by 2-fold ($p < 0.01$) and 4.5-fold ($p < 0.0001$), respectively (Figure 4A,B). In contrast to Animal 1, Animal 2 did not produce a dose-dependent response. A dose of 10 nmol/mL of Pam_2Cys induced the highest level of IL-6 at an 8.5-fold increase ($p < 0.05$) in the monolayers from Animal 2 (Figure 4A). Conversely, 1 nmol/mL of Pam_2Cys caused a 25-fold surge ($p < 0.001$) in IL-8 secretion in the monolayers from Animal 2 (Figure 4B). Although 5 and 10 nmol/mL of Pam_2Cys maintained significantly high levels of IL-8 ($p < 0.001$), they did not further elevate the production of IL-8 (Figure 4B).

To quantify the polarised secretion of IL-6 triggered by Pam_2Cys stimulation, supernatants obtained from the BME2 organoids 24 h post-stimulation were also analysed. Hydrocortisone (HCT) is a constituent of cell culture media that is used for growing organoids from airway epithelial cells. It supports the development and function of transepithelial ion transport proteins, which are critical for effective mucociliary clearance [41]. To our surprise, HCT inhibited IL-6 production by bovine tracheal organoids. IL-6 production was restored when organoids were weaned off HCT three days prior to Pam_2Cys stimulation. Like the monolayers, exposing BME2 organoids grown from Animal 1 to 1 nmol/mL of Pam_2Cys increased IL-6 level by 2.5-fold ($p < 0.05$) as compared to the untreated control. However, unlike the monolayers, stimulation of BME2 organoids from Animal 2 only resulted in a minor non-significant increase in IL-6 expression.

Tracheal antimicrobial peptide (TAP) is a β-defensin which forms the first line of defence against respiratory pathogens and is generated by the mucosal epithelial cells of cattle [42]. To determine the effect of Pam_2Cys on *TAP* expression, we stimulated the BME2 organoids with 10 nmol/mL of Pam_2Cys and harvested the organoids after 6 h and 24 h for RT-qPCR analysis. *TAP* expression (primer sequences are listed in Table 1) was markedly upregulated (almost 5-fold, $p < 0.01$) and plateaued at 6 h post-stimulation (Figure 4D), indicating that Pam_2Cys can induce efficient and effective antimicrobial activity.

3.4. Effect of Pam_2Cys on BHV-1 Infection In Vitro

The bovine tracheal cell monolayers and organoids were treated with various concentrations of Pam_2Cys for 24 h before being infected with both the BHV-1 vaccine strain and the field isolate. Supernatants were harvested at 24 h post-infection (hpi) and 48 hpi for assessing viral titres by plaque assay. Figure 5 demonstrates that Pam_2Cys had minimal to no effect on suppressing the field isolate of BHV-1 (or vaccine strain, data not shown), either in the monolayers (Figure 5A) or the BME2 organoids (Figure 5B). The Pam_2Cys compound was validated with mass spectrometry (Figure S3) and its stimulatory effect on TLR2 signalling was confirmed by HEK-Blue hTLR2 assay (Figure S4). This suggests that the innate immune response in tracheal epithelial cells alone was insufficient to inhibit BHV-1 replication.

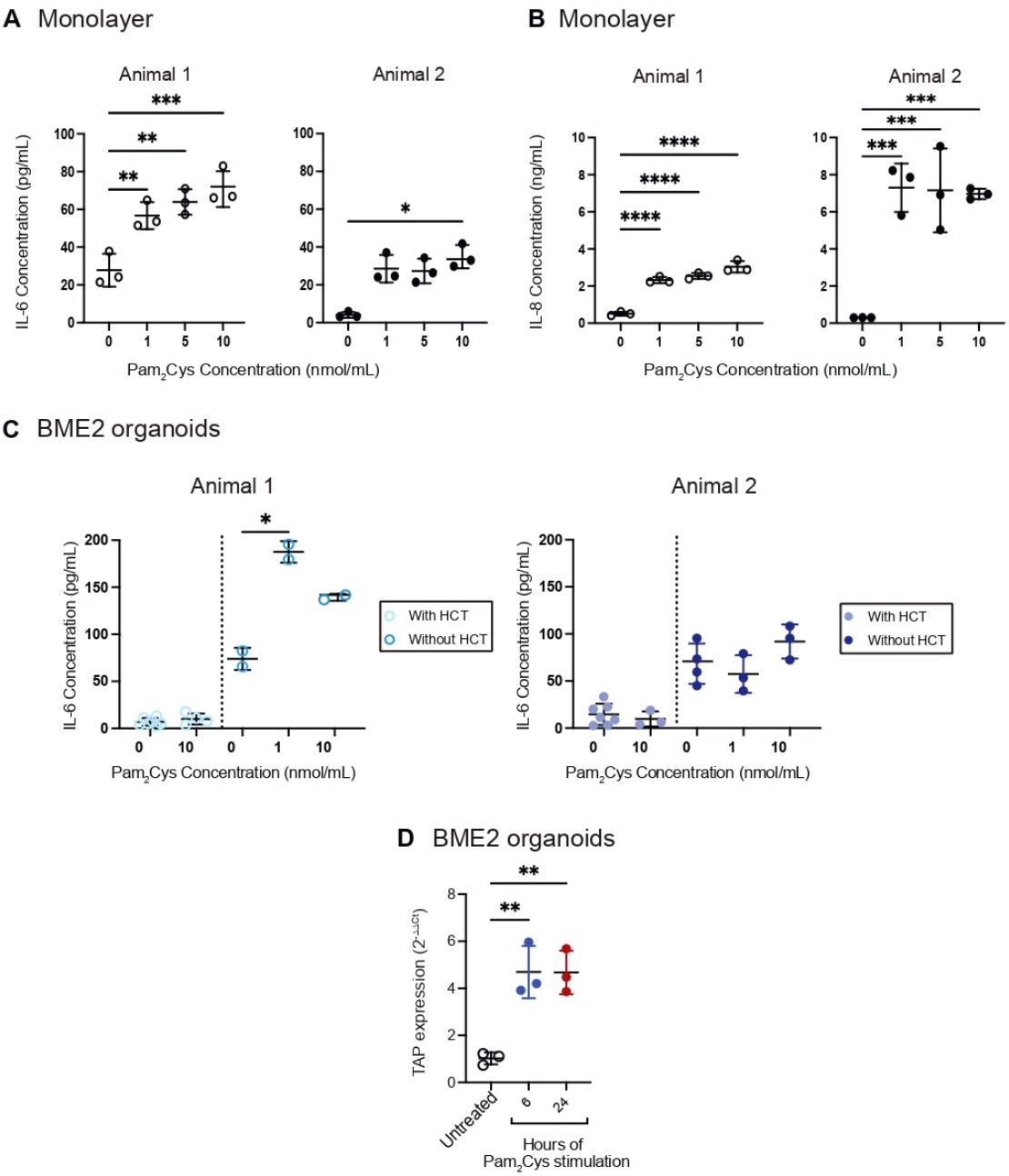

Figure 4. The effect of Pam_2Cys on the production of IL-6, IL-8 and *TAP*. Monolayers established from Animal 1 (**left**) and Animal 2 (**right**) were stimulated with Pam_2Cys at 1, 5 and 10 nmol/mL. (**A**) IL-6 and (**B**) IL-8 levels were assessed at 24h post-stimulation. (**C**) BME2 bovine tracheal organoids were grown from Animal 1 (**left**) and Animal 2 (**right**) and stimulated with Pam_2Cys in the presence or absence of HCT. IL-6 levels in the supernatants were measured using ELISA. (**D**) RT-qPCR analysis for expression level of *TAP* in BME2 organoids. Data represent mean ± standard deviation of two to seven technical replicates. Statistical analysis was performed using one-way ANOVA followed by Dunnett's ((**A**) left, (**B**,**C**) right and (**D**)) or Dunnett's T3 ((**C**) left) multiple comparison tests; or the Kruskal–Wallis test with Dunn's post hoc test ((**A**) right). * $p < 0.05$, ** $p < 0.01$, *** $p < 0.001$, **** $p < 0.0001$.

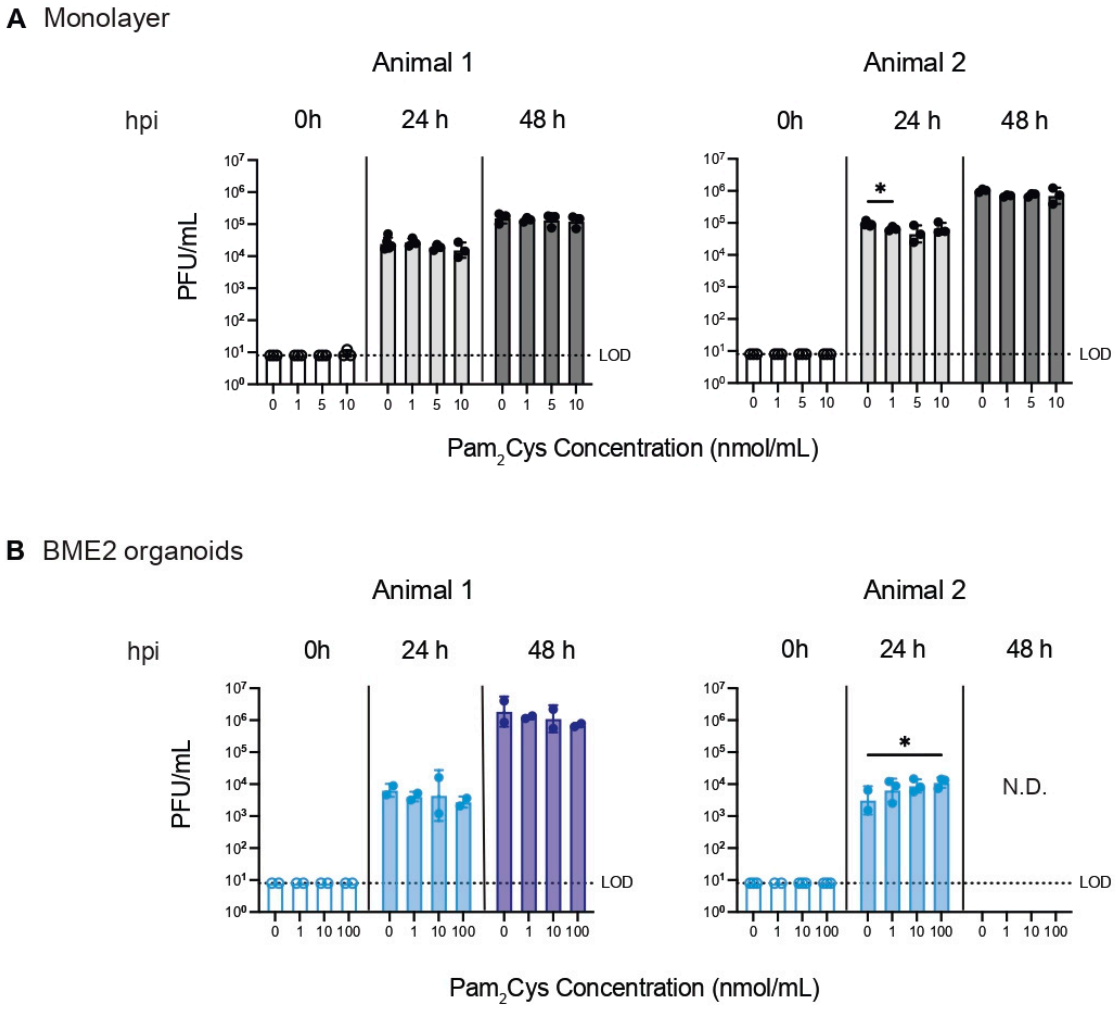

Figure 5. The effect of Pam_2Cys on the replication of BHV-1 field isolate. (**A**) Monolayer and (**B**) organoid cultures were established from bovine tracheal cells and treated with various concentrations of Pam_2Cys for 24 h prior to BHV-1 infection. Pam_2Cys stimulation and BHV-1 infection were carried out in the absence of HCT. Supernatants were harvested at time zero (T0), and 24 h and 48 h post-infection. Viral titres were assessed by performing the plaque assay. Data represent mean ± standard deviation of two to six technical replicates. Statistical analysis was performed using two-way ANOVA followed by Dunnett's multiple comparison test. * $p < 0.05$. BHV-1, bovine herpesvirus-1; HCT, hydrocortisone; hpi, hours post-infection; LOD, limit of detection; N.D., not determined; PFU, plaque forming unit.

4. Discussion

BRD is a major health problem faced by the beef industry worldwide where feedlot-based beef production is practiced, and is associated with economic losses of up to $AUD 40 million annually in Australia alone [43]. Understanding the host–pathogen interaction has been hampered by the need for tissue culture-based models that accurately model bovine respiratory physiology. Having previously established and optimised conditions for differentiation of human nasal epithelium [31], the aim of the present study was to similarly develop and characterise 3D differentiated organoids from bovine tracheal cells.

To achieve this, we established and optimised protocols to differentiate tracheal epithelia at the ALI and embedded in a BME2 matrix. Single-cell transcriptomic analysis revealed that both differentiation conditions yielded multiple differentiated respiratory epithelial cell types, including ciliated and mucosal cells. The UMAP plots showed that ALI- and matrix-differentiated clusters were distinct from the undifferentiated cells. The

overall UMAP distribution of ALI- and matrix-differentiated cells were similar, but numerical (cell density) differences were noted. The presence of differentiated cell types was confirmed by the expression of cell-type-specific proteins, using immunofluorescence confocal microscopy and ultra-structural features, using transmission electron microscopy. While we were able to generally assign cell types to our clusters, we note that there are limitations in using homologues as gene markers for cell cluster assignment. Therefore, further work is required to define cell-specific markers in the airway epithelia of cattle to visualise differences at a higher resolution.

Next, we showed for the first time that the 3D-matrix-differentiated organoids were susceptible to infection by the vaccine strain and field isolate strain of BHV-1. We chose BHV-1 as our pathogen of interest, as in most cases of BRD, it is BHV-1 that is associated with respiratory disease [4]. To the best of our knowledge, only one research team has successfully infected bovine airway epithelial cells grown at the ALI with BHV-1 [17]. The BME2 organoids that we established in this study offer an alternative polarised culture system that can be used to study the BHV-1 host–pathogen interaction without the need for a permeable support system.

In this study, we investigated the effect of Pam_2Cys on the induction of innate immune mediators including *TAP*, IL-6 and IL-8. Consistent with a previous study using bovine tracheal monolayer cultures [11], we observed that TLR2 activation also resulted in the upregulation of *TAP* gene expression in bovine tracheal 3D culture. In addition, Pam_2Cys stimulated IL-6 (cytokine) and IL-8 (chemokine) secretion by the tracheal epithelium cells when cultured as a monolayer and promoted IL-6 production by the tracheal organoids embedded in the matrix. Overall, our results agree with earlier studies [14,15] in mouse models that Pam_2Cys stimulates innate immune responses. This suggests that it can be used as an antimicrobial or antiviral agent against bovine respiratory disease.

Interestingly, we observed that addition of hydrocortisone (HCT) inhibited Pam_2Cys-mediated IL-6 production, which was restored when the glucocorticoid was removed from the media three days prior to Pam_2Cys treatment. It should be noted that HCT is routinely added to differentiation media for culturing airway organoids, to support the ion transport pathways at the apical border of differentiated airway epithelial cells. The roles of HCT include modulating the translocation and density of sodium channels, the transcription of cystic fibrosis transmembrane conductance regulator and β2-adrenergic receptor, and activation of large-conductance Ca^{2+}-activated K^+ channel by purinergic receptor agonists in ciliated cells [41,44]. This observation highlights the need for researchers to consider the effect of glucocorticoids on immune responses when using organoid models. In support of this notion, dexamethasone, which is the synthetic version of HCT, has been shown to suppress LPS-induced *TAP* expression in bovine tracheal epithelial cell cultures, but it did not affect LPS-induced lingual antimicrobial peptide (*LAP*) expression in a similar culture [30].

We have previously demonstrated in a mouse model of influenza infection that pre-treatment of the animals intranasally with Pam_2Cys inhibited viral replication by inducing an innate antiviral immune response through activation of cytokines, chemokines and immune cell infiltration [15]. Surprisingly, Pam_2Cys pre-treatment did not affect BHV-1 replication in either the monolayer or the matrix-embedded culture systems. Collectively, these findings indicate that cell-intrinsic antiviral mechanisms induced by the immunostimulant Pam_2Cys do not inhibit viral replication when activated in isolation. This implicates a role for the non-epithelial cellular microenvironment in vivo, as the bovine tracheal cultures comprise only epithelial cells. A previous study [45] reported that pro-inflammatory cytokines produced by BHV-1-infected bovine bronchial epithelial cells altered the adherence and migration of polymorphonuclear neutrophils. This suggests that interaction between the airway epithelial cells and the infiltrating innate immune cells is required to elicit an antiviral response after exposure to Pam_2Cys. Understanding the role of infiltrating innate immune cells requires further studies with more complex organoid models or live cattle.

In conclusion, we have established and characterised in vitro tracheal epithelium organoid models that we differentiated at the ALI and embedded in a matrix. We demonstrated that the matrix-embedded organoids support infection by vaccine and field BHV-1 isolates and provide insight into the epithelial cellular response to infection. Single-cell transcriptomic analysis of the undifferentiated and differentiated cells revealed that the cell types generated in the matrix-embedded protocol were more transcriptionally diverse compared to the undifferentiated cells and comparable to the cell types generated from ALI differentiation, highlighting the applicability of the matrix-embedded model for future research.

Supplementary Materials: The following supporting information can be downloaded at: https://www.mdpi.com/article/10.3390/organoids2020007/s1, Figure S1: Bovine tracheal epithelial organoids differentiation; Figure S2: Single-cell transcriptomic analysis identifying bovine organoid cell types in Pam2Cys-treated ALI organoid, untreated ALI organoid and BME2 organoid; Figure S3: Mass spectrometry validation of Pam2Cys; Figure S4: HEK-Blue™ hTLR2 assay of investigated Pam_2Cys compound at serial dilution concentrations for stimulatory effect on TLR2 signalling; Video S1: Beating cilia 1; Video S2: Beating cilia 2.

Author Contributions: Conceptualisation, G.D., D.C.J., P.C.R., P.S.Q., B.M.T., E.V. and L.J.M.C.; methodology, P.S.Q., B.M.T., C.Y.W., A.D.-M., C.A.H., V.D.A.C., J.J.-Y.C., L.J.M.C., E.V. and G.D.; software, P.S.Q., B.M.T., V.D.A.C., J.J.-Y.C. and L.J.M.C.; validation, P.S.Q., B.M.T., J.J.-Y.C. and W.Z.; formal analysis, P.S.Q., B.M.T. and V.D.A.C.; investigation, P.S.Q., B.M.T., V.D.A.C., C.Y.W., E.H., Z.T.; resources, L.J.M.C., D.C.J., P.C.R. and E.V.; data curation, P.S.Q., B.M.T., V.D.A.C., E.H. and Z.T.; writing—original draft preparation, P.S.Q. and B.M.T.; writing—review and editing, P.S.Q., B.M.T., J.J.-Y.C., E.V. and G.D.; visualisation, P.S.Q., B.M.T. and V.D.A.C.; supervision, L.J.M.C., D.C.J., E.V., P.C.R. and G.D.; project administration, P.S.Q., B.M.T., E.V. and G.D.; funding acquisition, L.J.M.C., D.C.J., P.C.R., G.D. and E.V. All authors have read and agreed to the published version of the manuscript.

Funding: This research was funded by an Australian Research Council Discovery Project grant, DP200102090, awarded to D.C.J., P.C.R. and G.D. B.M.T.'s salary was supported by a National Health and Medical Research Council of Australia (NHMRC) Ideas grant (APP1181580) awarded to E.V. and B.M.T. The funders had no role in the design of the study; in the collection, analysis or interpretation of data; in the writing of the manuscript; or in the decision to publish the results.

Institutional Review Board Statement: Not applicable.

Informed Consent Statement: Not applicable.

Data Availability Statement: Raw transcriptomic data will be made available once article is accepted for publication.

Acknowledgments: We are very grateful to Neil Charman (Gippsland Research Station Pty Ltd.) for his veterinary expertise and guidance. We thank Jiyoti Verma for her support with the Parse Evercode™ single-cell technology. We also thank the Biological Optical Microscopy Platform (BOMP) and the Melbourne Histology Platform for their enthusiastic assistance.

Conflicts of Interest: Pam_2Cys compound used for the research in this publication is the subject of the following patent applications owned by Ena Therapeutics: PCT/AU2011/001225 (D.C.J.), PCT/AU2018/051397 (D.C.J. and W.Z.), PCT/AU2018/051401 (D.C.J., G.D. and C.Y.W.) and PCT/AU2020/050660 (W.Z. and D.C.J.). D.C.J. is a consultant for Ena Respiratory.

References

1. ALFA. Feedlot Qtrly Survey Results. ALFA: Sydney, Australia. Available online: https://www.feedlots.com.au/news/categories/feedlot-qtrly-survey-results (accessed on 1 May 2023).
2. Gaudino, M.; Nagamine, B.; Ducatez, M.F.; Meyer, G. Understanding the mechanisms of viral and bacterial coinfections in bovine respiratory disease: A comprehensive literature review of experimental evidence. *Vet. Res.* **2022**, *53*, 70. [CrossRef] [PubMed]
3. Taylor, J.D.; Fulton, R.W.; Lehenbauer, T.W.; Step, D.L.; Confer, A.W. The epidemiology of bovine respiratory disease: What is the evidence for predisposing factors? *Can. Vet. J.* **2010**, *51*, 1095–1102. [PubMed]
4. Hay, K.; Barnes, T.; Morton, J.; Gravel, J.; Commins, M.; Horwood, P.; Ambrose, R.; Clements, A.; Mahony, T. Associations between exposure to viruses and bovine respiratory disease in Australian feedlot cattle. *Prev. Vet. Med.* **2016**, *127*, 121–133. [CrossRef]

5. Biswas, S.; Bandyopadhyay, S.; Dimri, U.; Patra, P.H. Bovine herpesvirus-1 (BHV-1)—A re-emerging concern in livestock: A revisit to its biology, epidemiology, diagnosis, and prophylaxis. *Vet. Q.* **2013**, *33*, 68–81. [CrossRef] [PubMed]
6. Pastenkos, G.; Lee, B.; Pritchard, S.M.; Nicola, A.V. Bovine Herpesvirus 1 Entry by a Low-pH Endosomal Pathway. *J. Virol.* **2018**, *92*, e00839-18. [CrossRef]
7. Cusack, P.M. *Bovine Respiratory Disease Preventive Practices Handbook*; Meat & Livestock Australia: North Sydney, Australia, 2022.
8. Srikumaran, S.; Kelling, C.L.; Ambagala, A. Immune evasion by pathogens of bovine respiratory disease complex. *Anim. Health Res. Rev.* **2007**, *8*, 215–229. [CrossRef]
9. Beutler, B.A. TLRs and Innate Immunity. *Blood* **2009**, *113*, 1399–1407. [CrossRef]
10. Kawasaki, T.; Kawai, T. Toll-like receptor signaling pathways. *Front. Immunol.* **2014**, *5*, 461. [CrossRef]
11. Berghuis, L.; Abdelaziz, K.T.; Bierworth, J.; Wyer, L.; Jacob, G.; Karrow, N.A.; Sharif, S.; Clark, M.E.; Caswell, J.L. Comparison of innate immune agonists for induction of tracheal antimicrobial peptide gene expression in tracheal epithelial cells of cattle. *Vet. Res.* **2014**, *45*, 105. [CrossRef]
12. Mühlradt, P.F.; Kiess, M.; Meyer, H.; Süssmuth, R.; Jung, G. Isolation, structure elucidation, and synthesis of a macrophage stimulatory lipopeptide from Mycoplasma fer-mentans acting at picomolar concentration. *J. Exp. Med.* **1997**, *185*, 1951–1958. [CrossRef]
13. Takeuchi, O.; Kawai, T.; Mühlradt, P.F.; Morr, M.; Radolf, J.D.; Zychlinsky, A.; Takeda, K.; Akira, S. Discrimination of bacterial lipoproteins by Toll-like receptor 6. *Int. Immunol.* **2001**, *13*, 933–940. [CrossRef]
14. Tan, A.C.L.; Mifsud, E.J.; Zeng, W.; Edenborough, K.; McVernon, J.; Brown, L.; Jackson, D.C. Intranasal Administration of the TLR2 Agonist Pam2Cys Provides Rapid Protection against Influenza in Mice. *Mol. Pharm.* **2012**, *9*, 2710–2718. [CrossRef]
15. Deliyannis, G.; Wong, C.Y.; McQuilten, H.A.; Bachem, A.; Clarke, M.; Jia, X.; Horrocks, K.; Zeng, W.; Girkin, J.; Scott, N.E.; et al. TLR2-mediated activation of innate responses in the upper airways confers antiviral protection of the lungs. *J. Clin. Investig.* **2021**, *6*, e140267. [CrossRef]
16. Burucua, M.M.; Quintana, S.; Lendez, P.; Cobo, E.R.; Ceriani, M.C.; Dolcini, G.; Odeón, A.C.; Pérez, S.E.; Marin, M.S. Modulation of cathelicidins, IFNbeta and TNFalpha by bovine alpha-herpesviruses is dependent on the stage of the infectious cycle. *Mol. Immunol.* **2019**, *111*, 136–144. [CrossRef]
17. Kirchhoff, J.; Uhlenbruck, S.; Goris, K.; Keil, G.M.; Herrler, G. Three viruses of the bovine respiratory disease complex apply different strategies to initiate infection. *Vet. Res.* **2014**, *45*, 20. [CrossRef]
18. Rosales, J.J.; Verna, A.; Marin, M.; Pérez, S. Bovine alphaherpesvirus type 5 replicates more efficiently than bovine alphaherpesvirus type 1 in undifferentiated human neural cells. *Virus Res.* **2020**, *286*, 198037. [CrossRef]
19. Taha-Abdelaziz, K.; Wyer, L.; Berghuis, L.; Bassel, L.L.; Clark, M.E.; Caswell, J.L. Regulation of tracheal antimicrobial peptide gene expression in airway epithelial cells of cattle. *Vet. Res.* **2016**, *47*, 44. [CrossRef]
20. Tran, B.M.; Deliyannis, G.; Hachani, A.; Earnest, L.; Torresi, J.; Vincan, E. Organoid Models of SARS-CoV-2 Infection: What Have We Learned about COVID-19? *Organoids* **2022**, *1*, 2–27. [CrossRef]
21. Alling, C.R.; Liu, C.-C.; Langohr, I.M.; Haque, M.; Carter, R.T.; Baker, R.E.; Lewin, A.C. Assessment of Cidofovir for Treatment of Ocular Bovine Herpesvirus-1 Infection in Cattle Using an Ex-Vivo Model. *Viruses* **2021**, *13*, 2102. [CrossRef]
22. Niesalla, H.; Dale, A.; Slater, J.; Scholes, S.; Archer, J.; Maskell, D.; Tucker, A. Critical assessment of an in vitro bovine respiratory organ culture system: A model of bovine herpesvirus-1 infection. *J. Virol. Methods* **2009**, *158*, 123–129. [CrossRef]
23. Cozens, D.; Grahame, E.; Sutherland, E.; Taylor, G.; Berry, C.C.; Davies, R.L. Development and optimization of a differentiated airway epithelial cell model of the bovine respiratory tract. *Sci. Rep.* **2018**, *8*, 853. [CrossRef] [PubMed]
24. Cozens, D.; Sutherland, E.; Marchesi, F.; Taylor, G.; Berry, C.C.; Davies, R.L. Temporal differentiation of bovine airway epithelial cells grown at an air-liquid interface. *Sci. Rep.* **2018**, *8*, 14893. [CrossRef] [PubMed]
25. Clevers, H. Modeling Development and Disease with Organoids. *Cell* **2016**, *165*, 1586–1597. [CrossRef] [PubMed]
26. Heo, J.H.; Kang, D.; Seo, S.J.; Jin, Y. Engineering the Extracellular Matrix for Organoid Culture. *Int. J. Stem Cells* **2022**, *15*, 60–69. [CrossRef]
27. Collett, S.; Torresi, J.; Silveira, L.E.; Truong, V.K.; Christiansen, D.; Tran, B.M.; Vincan, E.; Ramsland, P.A.; Elbourne, A. Investigating virus–host cell interactions: Comparative binding forces between hepatitis C virus-like particles and host cell receptors in 2D and 3D cell culture models. *J. Colloid Interface Sci.* **2021**, *592*, 371–384. [CrossRef]
28. Quintana, A.M.; Landolt, G.A.; Annis, K.M.; Hussey, G.S. Immunological characterization of the equine airway epithelium and of a primary equine airway epithelial cell culture model. *Vet. Immunol. Immunopathol.* **2011**, *140*, 226–236. [CrossRef]
29. Hussey, G.S.; Ashton, L.V.; Quintana, A.M.; Lunn, D.; Goehring, L.S.; Annis, K.; Landolt, G. Innate immune responses of airway epithelial cells to infection with Equine herpesvirus-1. *Vet. Microbiol.* **2014**, *170*, 28–38. [CrossRef]
30. Mitchell, G.B.; Al-Haddawi, M.H.; Clark, M.E.; Beveridge, J.D.; Caswell, J.L. Effect of Corticosteroids and Neuropeptides on the Expression of Defensins in Bovine Tracheal Epithelial Cells. *Infect. Immun.* **2007**, *75*, 1325–1334. [CrossRef]
31. Tran, B.M.; Grimley, S.L.; McAuley, J.L.; Hachani, A.; Earnest, L.; Wong, S.L.; Caly, L.; Druce, J.; Purcell, D.F.J.; Jackson, D.C.; et al. Air-Liquid-Interface Differentiated Human Nose Epithelium: A Robust Primary Tissue Culture Model of SARS-CoV-2 Infection. *Int. J. Mol. Sci.* **2022**, *23*, 835. [CrossRef]
32. Deprez, M.; Zaragosi, L.-E.; Truchi, M.; Becavin, C.; García, S.R.; Arguel, M.-J.; Plaisant, M.; Magnone, V.; Lebrigand, K.; Abelanet, S.; et al. A Single-Cell Atlas of the Human Healthy Airways. *Am. J. Respir. Crit. Care Med.* **2020**, *202*, 1636–1645. [CrossRef]

33. Ravindra, N.G.; Alfajaro, M.M.; Gasque, V.; Huston, N.C.; Wan, H.; Szigeti-Buck, K.; Yasumoto, Y.; Greaney, A.M.; Habet, V.; Chow, R.D.; et al. Single-cell longitudinal analysis of SARS-CoV-2 infection in human airway epithelium identifies target cells, alterations in gene expression, and cell state changes. *PLoS Biol.* **2021**, *19*, e3001143. [CrossRef]
34. García, S.R.; Deprez, M.; Lebrigand, K.; Cavard, A.; Paquet, A.; Arguel, M.-J.; Magnone, V.; Truchi, M.; Caballero, I.; Leroy, S.; et al. Novel dynamics of human mucociliary differentiation revealed by single-cell RNA sequencing of nasal epithelial cultures. *Development* **2019**, *146*, dev.177428. [CrossRef]
35. Flanagan, D.J.; Phesse, T.J.; Barker, N.; Schwab, R.H.M.; Amin, N.; Malaterre, J.; Stange, D.E.; Nowell, C.J.; Currie, S.A.; Saw, J.T.S.; et al. Frizzled7 Functions as a Wnt Receptor in Intestinal Epithelial Lgr5+ Stem Cells. *Stem Cell Rep.* **2015**, *4*, 759–767. [CrossRef]
36. Brake, F.; Studdert, M.I. Molecular epidemiology and pathogenesis of ruminant herpesviruses including bovine, buffalo and caprine herpesviruses 1 and bovine encephalitis herpesvirus. *Aust. Vet. J.* **1985**, *62*, 331–334. [CrossRef]
37. Hanssen, E.; Dekiwadia, C.; Riglar, D.T.; Rug, M.; Lemgruber, L.; Cowman, A.F.; Cyrklaff, M.; Kudryashev, M.; Frischknecht, F.; Baum, J.; et al. Electron tomography of Plasmodium falciparum merozoites reveals core cellular events that underpin erythrocyte invasion. *Cell Microbiol.* **2013**, *15*, 1457–1472. [CrossRef]
38. Snowdon, W.A. Infectious bovine rhinotracheitis and infectious pustular vulvovaginitis in aus-tralian cattle. *Aust. Vet. J.* **1964**, *40*, 277–288. [CrossRef]
39. Velazquez-Salinas, L.; Verdugo-Rodriguez, A.; Rodriguez, L.L.; Borca, M.V. The Role of Interleukin 6 During Viral Infections. *Front. Microbiol.* **2019**, *10*, 1057. [CrossRef]
40. Mukaida, N.; Harada, A.; Matsushima, K. Interleukin-8 (IL-8) and monocyte chemotactic and activating factor (MCAF/MCP-1), chemokines essentially involved in inflammatory and immune reactions. *Cytokine Growth Factor Rev.* **1998**, *9*, 9–23. [CrossRef]
41. Zaidman, N.A.; Panoskaltsis-Mortari, A.; O'Grady, S.M. Differentiation of human bronchial epithelial cells: Role of hydrocortisone in development of ion transport pathways involved in mucociliary clearance. *Am. J. Physiol. Physiol.* **2016**, *311*, C225–C236. [CrossRef]
42. Kumar, R.; Ali, S.A.; Singh, S.K.; Bhushan, V.; Mathur, M.; Jamwal, S.; Mohanty, A.K.; Kaushik, J.K.; Kumar, S. Antimicrobial Peptides in Farm Animals: An Updated Review on Its Diversity, Function, Modes of Action and Therapeutic Prospects. *Vet. Sci.* **2020**, *7*, 206. [CrossRef]
43. Barnes, T.; Hay, K.; Morton, J.; Mahony, T. *Epidemiology and Management of Bovine Respiratory Disease in Feedlot Cattle: Final Report for Project B.FLT.0225*; Meat & Livestock Australia: North Sydney, Australia, 2015.
44. Zaidman, N.A.; Panoskaltsis-Mortari, A.; O'Grady, S.M. Large-conductance Ca2+-activated K+channel activation by apical P2Y receptor agonists requires hydrocortisone in differentiated airway epithelium. *J. Physiol.* **2017**, *595*, 4631–4645. [CrossRef] [PubMed]
45. Rivera-Rivas, J.J.; Kisiela, D.; Czuprynski, C.J. Bovine herpesvirus type 1 infection of bovine bronchial epithelial cells increases neutrophil adhesion and activation. *Vet. Immunol. Immunopathol.* **2009**, *131*, 167–176. [CrossRef] [PubMed]